Tutor/s

Dra. Maria Sarret Pons
Departament de Química Física

Dra. Montserrat Mitjans Arnal
Departament de Fisiologia

Grau de Química

Treball Final de Grau

In vitro safety assessment of nanomaterials: Protein corona studies on ZnO particles.

Estudi de la seguretat de nanomaterials _in vitro_: Estudis de la corona proteica en partícules de ZnO.

Marc Bilbao Asensio

Juny 2016

Universitat de Barcelona

B:KC Barcelona Knowledge Campus
Campus d'Excel·lència Internacional

What is past, is prologue.

William Shakespeare

El meu agraïment al grup de recerca ITMC, especialment a les doctores Montserrat Mitjans i Pilar Vilardell, pel seu consell, guia i supervisió durant el desenvolupament d'aquest estudi, i a la Dra Carmen Moran, pel seu recolzament diari al laboratori.

M'agradaria expressar, també, la meva gratitud a la Dra. Maria Sarret, pel seu consell i orientació al llarg de tot el procés, i a Joan Mendoza, de la unitat de Centres científics i Tecnològics de la Universitat de Barcelona, per la seva ajuda en les nostres observacions amb TEM.

Finalment, donar les gràcies als meus companys de laboratori: Glòria Somalo, Javier Carazo, Guillem Ruano i Ana Isa Predroso.

REPORT

CONTENTS

1. SUMMARY

Nanotechnology has been advancing relentlessly and the use of nanoparticles has increased rapidly as they have been applied in numerous industrial and medical sectors. For instance, Silver nanoparticles can be found in aerosols, Zinc and Titanium oxides are important components of sunscreen and applications of different nanoparticles have proved to be relevant in biomedicine as multifunctional drug carriers or in novel cancer therapies.

Nevertheless, potential dangers from nanoparticle exposure cannot be ignored. Nanoparticles may damage organisms. *In vitro*, studies have found certain nanoparticles to be able to break DNA helices, denaturalise vital proteins, disrupt gene expression or alter plasma coagulation. *In vivo*, they can induce inflammation and stimulate or suppress the immune system. Due to the ease of exposure to nanoparticles, the study and understanding of their potential toxicity is fundamental. The area of this research goes by the name of Nanotoxicology.

Herein, different sized particles of ZnO, characterized by different methods, were used to study their interaction with plasma proteins, both human and rat. Plasma proteome alteration, as a result of the presence of ZnO in different conditions, has been evaluated in order to gain knowledge of potential toxicity from these nanoparticles and its consequences.

Experimental results reported plasma coagulation delays, especially when studying the intrinsic coagulation pathway. Rat and human plasma were not equally affected by the ZnO particle's presence; SDS-PAGE gels revealed significant differences among proteins adsorbed on the particles depending on the organism studied. The formation of a proteic coating on ZnO particles, the protein corona, was confirmed through observations on TEM and consequent stabilization of particle dispersion was reported by DLS.

Keywords: ZnO nanoparticles, Nanotoxicity, Protein corona, Plasma coagulation, SDS-PAGE, TEM.

2. RESUM

La nanotecnologia avança sense aturador i l'ús de nanopartícules ha augmentat ràpidament degut a la seva aplicació en nombrosos sectors industrials i mèdics. Per exemple, es poden trobar nanopartícules de plata en aerosols, òxids de zinc i de titani en cremes solars, i s'han realitzat rellevants avenços en el camp de la biomedicina gràcies a l'aplicació de diferents nanopartícules com a portadors multifuncionals de fàrmacs, o en noves teràpies contra el càncer, entre d'altres.

No obstant, no es poden ignorar els potencials riscs de toxicitat davant l'exposició a aquestes nanopartícules, ja que poden danyar l'organisme. Estudis *in vitro* han observat com determinades nanopartícules són capaces de trencar l'hèlix d'ADN, desnaturalitzar proteïnes vitals, interrompre expressió genòmica o alterar la coagulació sanguínia. *In vivo*, aquestes poden causar inflamació o alterar el sistema immunitari. Degut a que les nanopartícules poden ser fàcilment trobades en productes disponibles al mercat, l'estudi i la comprensió del seu potencial tòxic és fonamental. L'àrea encarregada d'aquesta recerca s'anomena Nanotoxicologia.

En aquest estudi, nanopartícules de diferents mides de ZnO, caracteritzades mitjançant diferents mètodes, han estat usades per a estudiar la seva interacció amb plasma humà i de rata. L'alteració proteica, com a resultat de la presència de ZnO en diferents condicions, han sigut avaluades per tal d'adquirir coneixements sobre la potencial toxicitat d'aquestes nanopartícules i les seves conseqüències.

Els resultats experimentals obtinguts informen de retards en la coagulació del plasma, especialment en el camí intrínsec de la coagulació. Els plasmes de rata i home no es veien afectats de la mateixa manera en presència de les partícules de ZnO; els gels de SDS-PAGE revelaven diferències significatives entre les proteïnes adsorbides a les partícules depenent de l'organisme estudiat. La formació d'un embolcall proteic al voltant de les partícules de ZnO, la corona proteica, va ser confirmat mitjançant observacions en TEM, i la conseqüent estabilització de la dispersió de les partícules va ser observada mitjançant DLS.

Keywords: Nanoparticules ZnO, Nanotoxicitat, Corona proteica, Coagulació sanguínia, SDS-PAGE, TEM.

3. INTRODUCTION

3.1 NANOTECHNOLOGY AND NANOPARTICLES

Nanotechnology is defined, by the National Nanotechnology Initiative, as the manipulation of matter sized from 1 to 100 nanometers, known as Nanomaterials.

Nanoparticles (NPs) have been found to be useful in a wide variety of scientific and industrial areas. For instance, Silver NPs can be found in aerosols, Zinc and Titanium oxides are important components of sunscreen [1] and numerous NPs have proved to be relevant in biomedicine as multifunctional drug carriers or in novel cancer therapies [2]. Specifically, ZnO NPs have been found to apply as bactericides or anticarcinogenics [3], [4].

Unlike regular sized particles, NPs have high surface/volume ratios that increase as the nanoparticle size decreases [5]. That results in high reactivity with prominent physical properties and advantageous characteristics that are being used in several fields of science and industry.

Although it is encouraging for scientific research and innovation, NP's numerous applications throughout commercially available products, therefore their easy exposure to humans, have aroused concern for their potential toxicity. In fact, potential dangers from nanoparticle exposure have been reported: *In vitro*, certain nanoparticles are able to break DNA helices, denaturalise vital proteins, disrupt gene expression or alter plasma coagulation. *In vivo*, they can induce inflammation and stimulate or suppress the immune system [6]. A new science named Nanotoxicology was born to deal with this matter.

Different effects derived from nanoparticles have proven to be based on their size, their shape and curvature, their surface area, or their surface charge [7]–[9]. All these items regulate the affinity between the particle and the proteins in the media, thus conforming a dense cloud surrounding the particles of critical importance, called the Protein Corona.

3.2 PROTEIN CORONA

The biological activity of the nanoparticles is mainly based on the Protein Corona. When suspended, the nanoparticle interacts with the proteins in the media and binds them around itself. This process results in the total covering of the nanoparticle as shown in Figure 3.1.

Figure 3.1 *Representation of the Protein Corona. To the left, the nanoparticle alone. To the right, the nanoparticle in blood suspension all covered by proteins.*

The protein corona becomes the interface between the particle and the cellular system. Therefore, the nanoparticle-corona complex is the entity that represents "what the cell sees". It has been experimentally found that the biological activity originated by nanoparticles is based on the protein corona bound to them, and not on so much the bare characteristics of the particle itself [8].

As stated by the Vroman effect, we should expect the most mobile proteins to bind rapidly to the nanoparticle, and afterwards being replaced in equilibrium with other proteins of lower mobility and higher affinity to the particle [10]. Therefore, after a certain time of incubation, we could expect to divide the corona in two parts, the so called "Hard-corona", an inner layer formed by the proteins with highest affinity to the particle, and the "Soft-corona", formed of proteins of highest mobility and not so much affinity to the particles (Figure 3.2).

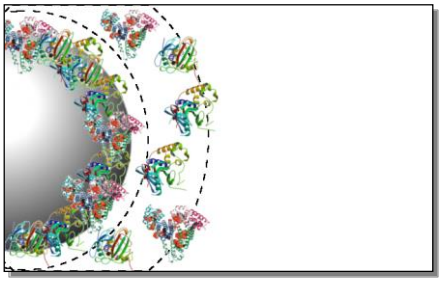

Figure 3.2 *Representation of the hard-corona, inner layer, and soft- corona, outer layer.*

The Vroman effect suggested that the biological activity could change through time. Nevertheless, this protein corona has been reported to be formed at <0.5 min. After that, although it was observed kinetic flowing of proteins in-and-out the corona, the corona did only change quantitatively and not qualitatively [8]. Thus, the biological activity remained the same, determined since the very first moment. That being said, the knowledge on the regulation of the protein corona is still limited.

Before further explanation of causes and consequences found in studies regarding the protein corona, essential information regarding the physiological media herein studied will be exposed in the following section.

3.3 PHYSIOLOGICAL MEDIA

Herein, our particles will be incubated in plasma, which is significantly different from blood or serum [11]:

1. Whole blood is a suspension of necessary nutrients, organic molecules, and cellular components (Erythrocytes, Leucocytes, Platelets…) immersed in aqueous media, plasma.
2. Plasma approximately consists of 55% of the whole blood volume. It is the aqueous media where blood cellular elements are immersed, which can be separated from it through centrifugation or sedimentation. Plasma is formed basically for water (91%), proteins (7%) and other solutes such as nutrients, electrolytes, etc.
3. Serum is collected after blood coagulation, centrifuged and separated from its cellular elements. Therefore, it is essentially plasma lacking blood coagulation factors and related proteins.

Possible consequences derived from NPs incubation will be studied through the evaluation of changes in plasma's behavior, such as alterations in blood coagulation, thus leading to the identification of the proteins affected.

3.3.1 Plasma Proteins

Human plasma contains approximately 1,200 different proteins [12], although a vast majority of which are found in an almost insignificant concentration. Table 3.1 describes the characteristics and functions of some of the most abundant of these proteins.

Protein	Characteristics	Functions
Albumin [13]	54% of plasma proteins MW=65kDa 4.5g/100ml	Transports poorly soluble molecules, binds toxic heavy metal ions, provides a reserve of protein and maintains plasma colloidal osmotic pressure.
α1-antitrypsin [13]	MW=45kDa 250mg/100ml	Responsible for nearly all the protease inhibiting capacity of serum
Fibrinogen [13]	MW=340kDa 300mg/100ml	Precursor of fibrin, the insoluble protein of blood clots
Protein C [14]	MW=62kDa 0.500mg/100ml	Regulates anticoagulation
Transferrin [13]	MW=80kDa 290mg/100ml	Transports iron
α2-macroglobulin [15]	MW=185kDa 1.2mg/ml [16]	Inhibits proteases (peptide bond breakers) that function in hemostatic and inflammatory reactions

Table 3.1. *General properties of some of the most abundant plasma proteins.*

3.3.2 Plasma Coagulation Assays

The core of our studies will be the process of Plasma Coagulation.

Plasma coagulation is the process by which blood generates a protective protein wall made of fibrin in order to prevent blood loss and haemorrhages. The development of this process depends on the action of several Coagulation Factors that are divided in two different pathways, depending on how the coagulation is activated: extrinsic pathway (studied through Prothrombin Time assays, PT), which is activated when a tissue has been injured; and intrinsic pathway (studied through Activated Partial Thromboplastin Time assays, APTT), activated when internal cells have been eroded or damaged. Both pathways eventually converge in a final Common pathway and are classically represented in the chain reaction known as the Coagulation Cascade, as seen in Figure 3.3 [17].

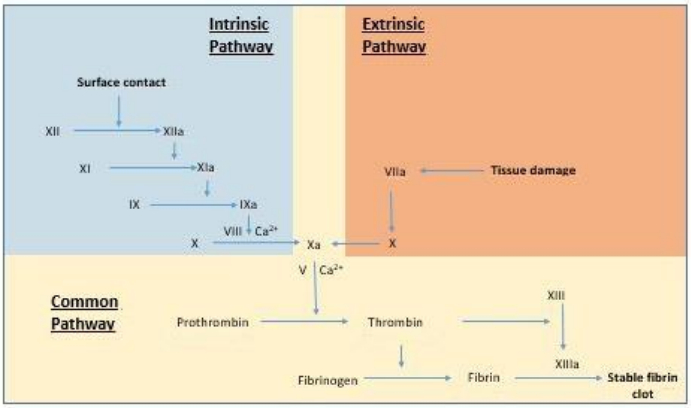

Figure 3.3 *Schematic representation of the Coagulation Cascade.*

As many other proteins, the factors inherent in this process have been found to interact with NPs and, due to protein conformational changes or deactivation, different consequences were observed. For instance, those NPs found to interact with Factor XII from the intrinsic pathway reported thrombosis induction (blood coagulation induction), whereas those NPs that interacted with Factor IV (Protein C, see Section 3.3.1, Table 3.1) were found to delay and obstruct thrombosis [18].

In that context, our studies will evaluate and compare changes of development of both pathways in both rat and human plasma as described in Section 5.4.

3.4 Previous Pathophysiological Studies

Pathophysiology, as a part of Pathology sciences, studies the mechanisms by which the organisms present altered physiological functions. As stated before, the presence of Nanoparticles in the organism results in an alteration of the proteins of the media when forming the protein corona, resulting in several consequences. Some of these studies reflect the importance of studying the effects of NPs in our organism:

- NPs are able to change the protein structure once they are bound. For instance, it has been reported that, when interacting with silver nanoparticles, the percent of α-helices from HAS (Human Serum Albumin: the most abundant protein in human plasma, essential for nutrient transportation among other functions) was reduced, whereas that of β-sheets was increased [19]. Meaning that protein functionality

could dangerously mutate, or even disappear, as the nanoparticle is able to denaturalise it.

- What is more, the protein corona may determine the path of the nanoparticles throughout the organism. It is able to modulate cellular uptake of the nanoparticles depending on the media they were pre-incubated in. For instance, after 2 hours of incubation of silver particles in a media containing albumin and IgG (common proteins found in Plasma), cellular uptake of the particles was reduced [19].

3.4.1 Previous Pathophysiological Studies Regarding ZnO NPs

Regarding the NPs from our studies, ZnO NPs, significant findings have already been reported, which will help us understand our experimental results:

- BSA (Bovine Serum Albumin, the biological behaviour of which is equivalent to Human's Albumin) mutates its secondary structure when interacts with ZnO NPs; the percentage of α-helices from the protein is reduced, whereas that of β-sheets is increased [20]. Thus meaning, as previously stated, that its functionality could be dangerously altered or deactivated in contact with NPs.
- ZnO causes a dose-dependent hemolytic activity (rupture of erythrocytes, red blood cells, that contain hemoglobin) activity. Although the exact mechanism remains unclear, data suggested that ZnO could enter into the cells and induce cell membrane rupture. <100nm NP reported the highest toxicity in these studies, inducing around 70% of hemolysis at concentrations of 0.2mg/ml (37ºC).

  In addition, it was observed how ZnO NPs could cause abnormal erythrocyte morphology when incubated for 3h (37ºC). Once again, <100nm NP caused the most significant morphological changes [21].
- ZnO caused significant dose-dependent plasma coagulation delays on human plasma when measuring both Intrinsic and Extrinsic pathways [21].

4. OBJECTIVES

The present study is focused on evaluating toxicity caused by zinc oxide particles on both human and plasma.

The aim of this study is four-fold:

1. To characterize ZnO particles with different methodologies.

2. To observe and compare the effect of zinc oxide particles on blood coagulation from both rat and human plasma.

3. To qualitatively assess differences in affinity among the different plasma proteins to ZnO particles.

4. To visually confirm the presence of protein corona through TEM.

5. EXPERIMENTAL SECTION

5.1 REAGENTS

5.1.1 General Reagents

ZnO nanopowder <50 nm particle size (Sigma-Aldrich, >97%)

ZnO nanopowder, <100 nm particle size (Sigma-Aldrich)

ZnO puriss. p.a., ACS reagent (Sigma-Aldrich, ≥99.0%),

PBS (Phosphate Buffered Saline): Potassium dihydrogen phosphate, extra pure (Scharlau), Sodium chloride, synthesis grade (Scharlau), di-Sodium hydrogen phosphate anhydrous (Panreac) at a concentration of 0.762 g/L, 7.056 g/L, 3.151 g/L, respectively, at pH=7.4.

EDTA (Farmitalia Carlo Erba, RPE-for analysis-ACS reagent)

Sodium Citrate p.a. (Sigma-Aldrich)

5.1.2 Plasma Coagulation Assay Reagents

Specific testing (Instrumentation Laboratory Co):

RecombiPlasTin 2G (RTF and RTF Diluent): is a liposomal preparation that contains human RTF (recombinant human tissue factor) relipidated in a synthetic phospholipid blend and combined with calcium chloride, buffer and a preservative.

SynthASil (ATTP Reagent – cephalin - and CaCl2): the ATTP is a liquid buffered reagent which contains synthetic phospholipid for optimal platelet-like activity and highly defined non-setting colloidal silica for optimal activation of the contact phase of coagulation.

5.1.3 Plasma Proteïn-ZnO Interaction Reagents

Bovine Serum Albumin (Sigma-Aldrich, ≥96%)

Coomassie brilliant blue G-250 (BioRad)

D(+)-Sucrose (Carlo Erba Reagents, RPE-for analysis-ACS)

Formic Acid (Scharlau, 85%)

Tris(hidroximetil)aminometà (Carlos Erga Reagents, RPE-for analysis)

Hydrochloric acid (Scharlau, 37%, Reagent Grade)

Sodium Dodecyl Sulfate (Sigma Aldrich, ≥98.5%)

Persulfat amònic (Amersham Biosciences, 98%)

Glycine (Scharlau, Reagent Grade, ACS)

Bromophenol blue (Amersham Biosciences)

b-mercaptotanol (Sigma Aldrich, ≥99%)

Comassie Brillant Blue R-250 (Serva)

Methanol (Scharlau, Reagent Grade)

Glacial Acetic Acid (Scharlau, Reagent grade)

Acrylamide PAGE (Amersham Biosciences, 40%)

Methylenebisacrylamide (Amersham Biosciences, 2%w/v)

N,N,N',N'-Tetramethyl-ethylenediamine (Sigma-Aldrich, 99%)

Phosphotungstic acid (2%, pH=6.4)

5.2 INSTRUMENTS

Centrifuge Megafuge 1.0 (Heraeus) and Centrifuge Biofuge Pico (Heraeus)

Centrifuge Nahita Blue 2624/2

Spectrophotometer Shimadzu UV-Vis 160

Rotary shaker and temperature controlled cabin.

Coagulometer Amleung KC 1A

SDS-PAGE: Mini PROTEAN 3 system (BIORAD)

Analytical Balance Sartorius CP1245

Sonicator Fungilab

Transmission Electron Microscopy (TEM) JEOL JEM LaB6-2100

Dynamic Light Scattering (DLS) Malvern Zetasizer Nano ZS

5.3 CARACTERIZATION OF ZnO NANOPARTICLES

Different properties of nanoparticles depend on parameters such as particle size, agglomeration (reflected on hydrodynamic diameter measures), particle charge, surface area or structural shape [8]. Therefore, in order to fully understand the behaviour of our nanoparticles throughout our study, it is essential characterize them.

5.3.1 General Properties

Properties	ZnO nanopowder <50 nm	ZnO nanopowder <100 nm	ZnO powder
Size	<50 nm	<100 nm	Micrometric
Color	White	White	White
Solubility	1.6mg/L (Water, 29ºC) [22]		
Molar Mass	81.41 g/mol		
Crystal structure	Hexagonal Wurtzite [5]		
Surface Charge	Negative (when suspended on PBS) [23]		
Abbreviation	<50nm NP	<100nm NP	Micro P

Table 5.1. *General properties from ZnO NP used in our studies. Information extracted from provider (Sigma-Aldrich) if not specifically referenced.*

As our study is the continuation of many others, our particles are, in part, already characterized. Herein it was studied the shape and structure of our particles through X-ray diffraction, and hydrodynamic diameter through light-scattering. Characterization by TEM had been partly studied in previous work, although deeper studies have been realized in order to be able to detect the protein corona (See Section 5.6).

5.3.2 X-Ray Characterization

Each ZnO nanoparticle was dispersed in PBS media and studied through X ray in order to understand their crystalline structure and recognize possible differences among different sized particles.

5.3.3 Anticoagulant

It is essential to control the stability of our particles in front of certain conditions inherent in our study. There will be used different blood anticoagulants (EDTA and Sodium citrate) through our analysis in order to prevent undesired plasma coagulation. Their effect is based on their ability to chelate the calcium present in our blood, which is essential to blood coagulation. Nevertheless, both anticoagulants are great chelants that could interact with our ZnO particles.

Studies were performed in order to recognize the anticoagulant that provides greater stability to the ZnO nanoparticles. Blank solutions of each anticoagulant with each nanoparticle were elaborated as described in Table 5.2. NP's and anticoagulant concentrations in these blank solutions were equivalent to those used in Plasma coagulation assays.

Entry	Study	PBS (μL)	NP's Solution (μL)	Total Volume (μL)	Final NP's Concentration (mg/ml)
1 & 4	<50nm ZnO	900	90	990	0.9
2 & 5	<100nm ZnO	900	90	990	0.9
3 & 6	Micro P ZnO	900	90	990	0.9

Table 5.2. *Composition of the blank solutions studied. Each NP solution was prepared from 0.0050g of the respective NP in 500 μL of PBS (10mg/ml), previously sonicated in order to prevent aggregation. Anticoagulant concentrations were 0.129M of sodium citrate for entries 1,2,3 and 2mg/ml of EDTA for entries 4,5,6.*

5.3.4 Hydrodynamic Diameter

There is a tendency from particles to aggregate when suspended, so this method measures de sizes of the clustered particles rather than individual particles [24]. As protein corona is known to be formed when particles are suspended in plasma, different results are expected to be reported depending upon the media used.

Each particle was suspended in PBS and citrated human plasma media as described in Table 5.3. Previous to measurement, particle control samples were sonicated. All samples were diluted 1:10 in MiliQ water in order to prevent further aggregation and potential measurement interferences. Measures contemplated ZnO's Refractive Index of 2.00.

Entry	Sample	Plasma (μL)	PBS (μL)	Stock particle solution (μL)	Total Volume (μL)	NP's Conc. (mg/ml)
1	<50nm ZnO control	-	900	90	990	0.9
2	<100nm ZnO control	-	900	90	900	0.9
3	Micro ZnO control	-	900	90	990	0.9
4	Plasma control	900	90	-	990	-
5	<50nm ZnO	900	-	90	990	0.9
6	<100nm ZnO	900	-	90	990	0.9
7	Micro ZnO	900	-	90	990	0.9

Table 5.3. *Composition of the solutions studied. Each stock particle solution was prepared from 0.0050g of the respective particle in 500 μL of PBS resulting in concentrations of 10mg/ml, previously sonicated to prevent aggregation.*

5.4 PLASMA COAGULATION ASSAYS

Plasma coagulation time was measured in order to study the effects of the presence of ZnO nanoparticles in both human and rat Plasma. Experimentation was based on pre-existing protocols [25]: Five different solutions were incubated at 37ºC, described at Table 5.4, for 30 minutes. Three of them were composed by Plasma plus different sizes of NP's (<50, <100 and micro) at a concentration of 0.9 mg/ml, the other two solutions were controls made from Plasma (Entry 1) and rat/human Plasma plus PBS (Entry 2).

Once incubated, different coagulation assays were performed in order to study both extrinsic and intrinsic coagulation pathways. A coagulometer was used for that matter.

Entry	Sample	Plasma (μL)	PBS (μL)	NP's Solution (μL)	Total Volume (μL)	Final NP's Concentration (mg/ml)
1	Plasma control	900	-	-	900	0
2	PBS control	900	90	-	990	0
3	<50nm ZnO	900	-	90	990	0.9
4	<100nm ZnO	900	-	90	990	0.9
5	Micro ZnO	900	-	90	990	0.9

Table 5.4. *Composition of the solutions studied, both controls and NP's samples. The same compositions were used for both human and rat Plasma. Each NP solution was prepared from 0.0050g of the respective NP in 500 μL of PBS (10mg/ml), previously sonicated to prevent aggregation.*

This coagulometer includes a chronometer in order to measure the clot formation time while maintaining the temperature of the samples at 37ºC. It uses a special reaction cuvette with a steel ball inside in which the sample is added, inclined in a certain angle. The cuvette is always rotating around its longitudinal axis while the steel ball is held fixed in one position in the cuvette through the action of a small magnet. With the addition of the last reagent, Plasma clotting starts and the chronometer is manually activated. When the clots finally form, the ball gets blocked in one position thus starting to rotate with the cuvette. The change of position of the steel ball is registered by an electromagnetic sensor that automatically stops the chronometer.

For extrinsic pathways studies, 100μL of each solution reacted with 200μL of calcic thromboplastin. Time measurement started once calcic thromboplastin was added.

For intrinsic pathways studies, 100μL of cephalin were added to 100μL of each solution and left to react for 2 minutes. Then, 100μL of CaCl2 were added and, instantly, time measurement started.

5.4.1 Statistical Considerations

Each assay was carried out individually, using three replicates for each sample. Human plasma assays were meant to be a mere test as they were already studied; only a couple of tests were performed. This was not the case for rat plasma assays, which were performed three times.

5.5 PLASMA PROTEIN-ZnO INTERACTION

In order to study the different proteins involved in the protein coronas, and possible differences between supernatant and pellet, SDS-PAGE experiments were performed.

5.5.1 Sample treatment

Samples with NP were centrifuged (13.000 rpm, 5 min.) in order to separate the pellet from the supernatant and study them separately. We only studied the first supernatant of each sample. The pellets were washed 3 times with a solution of Sucrose 0.7M in PBS. Sucrose allows the pellet to precipitate in a more visual way, thus increasing the ease of separation from the supernatant [8].

In these studies, bigger concentrations of protein are required (Read Section 5.5.2). It is expected that the concentration of protein from the hard corona is correlated to the concentration of the particles themselves. Therefore, herein is used a particle concentration 10 times bigger than in plasma coagulation tests in order to gain sensibility, as described in Table 5.5. Plasma and PBS controls prepared as in Entries 1 & 2 from Table 5.4 were always employed.

Entry	Study	Plasma (μL)	NP's Solution (μL)	Total Volume (μL)	Final NP's Concentration (mg/ml)
1	<50nm ZnO	900	90	990	9.0
2	<100nm ZnO	900	90	990	9.0
3	Micro ZnO	900	90	990	9.0

Table 5.5. *Composition of the NP's samples studied. The same compositions were used for both human and rat Plasma. Each NP solution was made from 0.0500g of the respective NP in 500 μL of PBS (100 mg/ml), previously sonicated to prevent aggregation.*

5.5.2 SDS-PAGE

SDS-PAGE stands for *Sodium Dodecyl Sulfate Polyacrylamide Gel Electrophoresis*. It is a technique widely used to separate different biological macromolecules, such as proteins, according to their different electrophoretic mobility. Proteins will be denaturalized (breaking of non-covalent bonds) through the addition of SDS (detergent). The same SDS charges the

proteins negatively as it bounds to them and it will make the proteins head to the anode of the cell. The electronic repulsion created by these negative charges flattens the shape of the proteins, thus eliminating any electrophoretic mobility differences caused by their shape. In addition, proteins will be denaturalized by heating them to 95ºC. 2-mercaptoethanol, a reducing agent of disulphide linkages, is also used to help denaturalizing the proteins in the sample. Finally, a tracking dye, bromophenol blue, is added to the samples. Unlike the proteins in the sample, this tracking dye can be seen (it is blue). Also, it has greater electrophoretic mobility than any of the compounds in the sample, so it helps keeping the pace of the experiment; when the tracking dye reaches the end of the gel, the electrophoresis is stopped.

Note that proteomic quaternary structures are based on non-covalent bonds between several subunits, complexed as a whole. Therefore, due to the strong reductant media, multi-subunit proteins are expected to be divided into every subunit that composes them. For instance, human fibrinogen (MW=340kDa) is broken into 3 main subunits: fibrinogen α, MW=66kDa; fibrinogen β, MW=52kDa ; fibrinogen γ, MW=46kDa [26].

Once protein samples are treated, they are disposed in different compartments in a Polyacrylamide gel, which is chemically inert. Our gels are 1mm thick. This gel is prepared maximum 24 hours before, as it can dry out and break.

The gel is divided in two parts: the stacking gel and the running gel, as represented in Figure 5.3. Their purposes are clearly different. The proteins are injected in the cavities formed in the stacking gel. Once injected, with a subtle potential of 60 volts for 10 minutes, the stacking gel stacks all the proteins at the same point, a starting line, so they all start to migrate at the same time. This starting line is where the two different gels meet.

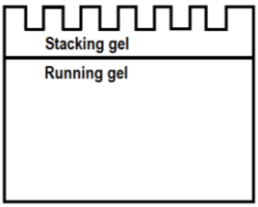

Figure 5.3. *Representation of SDS-PAGE gels.*

The difference between these two gels is based on their composition. The Stacking gel has a lower percentage of acrylamide (5%), which means larger pores, and is buffered at pH=6.8. Meanwhile, the Running gel has a higher percentage of acrylamide (7.5%), narrower pores, and

is buffered at pH=8.8, with different ionic content. The higher the pH, the higher negative charge bore by the proteins, thus making them more susceptible to the electrophoretic experiment.

At a greater potential of 200 volts, the proteins enter the running gel and the migration starts. The running gel allows the separation of the different proteins based on their molecular weight. As it is known: the greater the protein, the slower its movement through the pores of the gel. The process is illustrated in Figure 5.4.

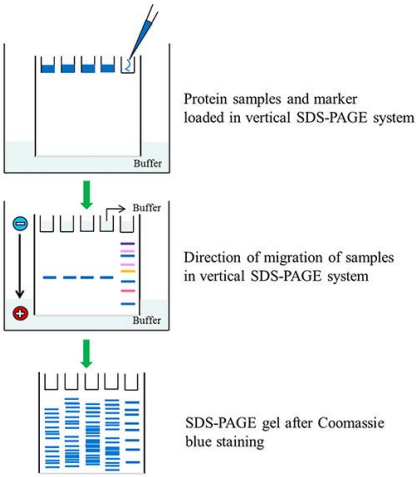

Figure 5.4. *Representation of SDS-PAGE experiments* [27].

A special highly pure protein solution will be injected in one of the cavities. This solution contains few proteins of different mass that will be also separated by electrophoresis. Once revealed, this solution will provide a reference, a clear pattern, of size of the proteins in the samples.

After electrophoresis, protein band stains are revealed when bathed in a solution of Comassie Brillant Blue R-250 (2.5g/L). Staining excess will be washed with a solution of methanol (7.5%) and Acetic acid (10%).

Nevertheless, the amount of protein in each cavity must be controlled. All cavities should bear the same absolute amount of proteins (10-30 μg), thus providing a clear separation of proteins so the different bands can be easily compared and studied. The Bradford method, used to analyse the concentrations of proteins in the samples, was previously performed for that matter (Section 5.5.3).

Herein, injected protein amounts were approximately of 18μg from plasma controls and supernatants (SNs). Total injected protein amounts from particle pellets varied as they were not capable of retaining enough protein (Amounts injected are indicated when discussing each assay). Experience demonstrated that it was possible to study the stain bands as they were clear and comparable enough, even though the optimal amount of protein was not reached and homogeneous amount of protein among the cavities from the same gel was not possible to accomplish as experimental injection is complicated and part of the protein sample is likely to be lost.

5.5.3 Bradford method

The Bradford assay is a photometric method that, through different absorbance among the samples, allows us to determine the amount of protein in them. It is based on the use of a colorant, Coomassie brilliant blue G-250, that when bound to proteins changes its red colour to blue.

From a stock solution of bovine albumin 1.5mg/ml, a standard analytical curve was designed as described in Table 5.6.

St. Solution	Stock sol. (μl)	PBS (μl)	Tot. Volume (μl)	Final Concentration (μg/ml)
1	50	1950	2000	37.5
2	100	1900	2000	75
3	200	1800	2000	150
4	400	1600	2000	300
5	666	1333	1999*	500
6	1000	1000	2000	750

Table 5.6. *Composition of the standard solutions of albumin used to calibrate the study. (*) It supposes an error of 0.05% that can be neglected.*

Supernatant and control solutions, due to their expected high protein concentration- confirmed by few primary tests- were diluted 80 times before analysis. PBS was used as blank solution.

Before final absorbance measurement, each sample, control and standard solution was treated as follows: 50μl of each sample were mixed with 50 μl of formic acid, and stirred. Then, 1.5 ml of colorant were added to the solution, and stirred. Colorant, BioRad's Coomassie blue, was diluted 1:5 before use. Absorbance measurement was performed at 595nm.

5.6 TEM STUDIES: PARTICLE CHARACTERIZATION AND PROTEIN CORONA

Through TEM (Transmission Electronic Microscopy), ZnO particles were observed when diluted in mere H2O (MiliQ quality) and when incubated in human plasma (also eventually suspended in MiliQ water) in order to visually characterize our NPs and detect the protein corona.

All samples were suspended in MiliQ water. Due to high particle aggregation, each control sample was diluted to contain 0.02μg/ml of each kind of particle respectively (<50nm NP, <100nm NP and Micro P) in order to adequately observe the particles. In contrast, each protein incubated particles sample was prepared at a preventive concentration of 0.9μg/ml (as Entries 3, 4 and 5 from Table 5.4 on Section 5.4) due to loss of pellet after following washing; particles apparently increased their solubility in the aqueous media after protein incubation.

All material was vigorously washed with MiliQ water in order to prevent sample contamination. Each sample was centrifuged and washed with MiliQ water at least 3 times. Measurements were made on a 5μl drop of sample left to dry over a Holey Carbon-Copper grid. Control samples were sonicated before measurement.

Proteins in our samples were revealed with phosphotungstic acid, which binds ionically to the positive charged groups, thus indicating whether protein was present or not around the particles. Phosphotungstic acid is electron dense and opaque to electron transmission, thus it is seen by TEM as dark staining. After drying the samples, a 5μl drop of phosphotungstic acid was added over the sample grid and then removed after 30 seconds. One last 5μl drop of water was added in order to eliminate potential excess of phosphotungstic acid, also removed after 30 seconds.

EDX (Energy-dispersive X-ray spectroscopy) analyses were performed to analyse the elemental composition of the sample, thus confirming the presence of plasma proteins, ZnO particles and the staining agent (tungsten, from the phosphotungstic acid).

TEM measurements were performed at the “Centres Científics i Tecnològics de la Universitat de Barcelona”.

6. ZnO PARTICLES CHARACTERIZATION: DISCUSSION

6.1 X-RAY SPECTROSCOPY

As seen in Figure 6.1, all three ZnO particles (Figure 6.1) share the same identical crystal system, thus meaning that no behavioural difference can be justified by structural differences among them. Moreover, they all hold the same ZnO's crystalline structure pattern (d), hexagonal wurtzite (JCPDS pattern), thus meaning that no anomalies or significant defects in the structure of the particles are to be expected.

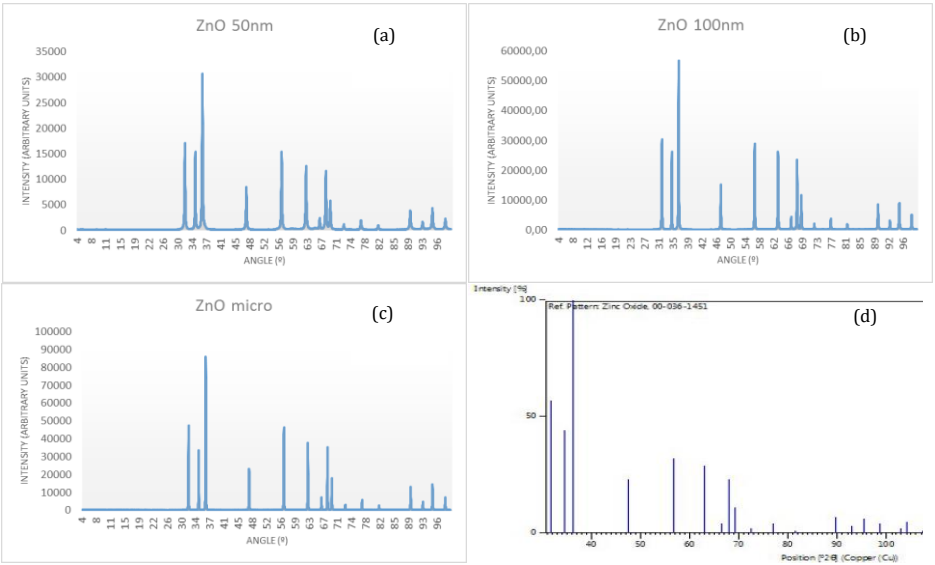

Figure 6.1. *Representation of X-Ray diffraction spectroscopy results for ZnO particles: (a) <50nm, (b) <100nm, (c) micro). (d) corresponds to ZnO structural pattern, a hexagonal cell.*

6.2 HYDRODYNAMIC DIAMETER

Our findings show differential behaviour of the ZnO particles depending upon the media used, as seen in Table 6.1.

Sample	Z-ave	Est. Desv.	PDI
<50nm ZnO control	2287	438.2	0.734
<100nm ZnO control	1940.8	233.0	0.729
Micro ZnO control	2448.2	1220.7	0.819
Plasma control	106.5	19.8	0.789
<50nm ZnO	166.1	4.6	0.188
<100nm ZnO	245.0	3.8	0.147
Micro ZnO	374.1	12.6	0.321

Table 6.1. *Hydrodynamic Diameters measured.*

Sizes measured from control samples are only qualitatively relevant due to the extremely high polydispersity index and standard deviation. It can be concluded that, when immersed in aqueous media, homogenic suspension is unstable and our particles quickly agglomerate and form random sized clusters.

In contrast, after being incubated in Plasma, our particles significantly reduced the tendency to agglomerate and polydispersity diminished up to ideal values (0.0 - 0.3; polydispersity indexes below 0.1 are referred to be monodispersed systems) [28]. Reasonable nanoparticle size could be measured - note that these measures include the size of the particle itself as well as the volume acquired when forming the protein corona.

Our findings already point out protein-NPs adsorption differences; Micro Ps still remain relatively polydispersed, much more than the other two NPs, thus meaning that their homogenic suspension has not been equally stabilized. Also, <50nm NP have relatively grown more from their initial sizing (from ≈30nm to ≈155.6nm, see Section 6.3) than <100 NPs (from ≈70nm to ≈245.0nm) and Micro P (due to initial size dispersion, it cannot be reliably compared, though size variation seems quite subtle as previous to incubation there can be already found bigger particles in the sample). These phenomena agree with our findings on Section 7.2, where the greatest protein adsorption is reported on <50 nm NPs, then <100nm NPs and lastly in Micro P.

6.3 TEM STUDIES: PARTICLE CHARACTERIZATION

In figure 6.2 can be observed the structure of our particles when immersed in MiliQ water. As expected, NPs form great agglomerations when immersed in aqueous media. The same figure represents the clearest spots found in our samples.

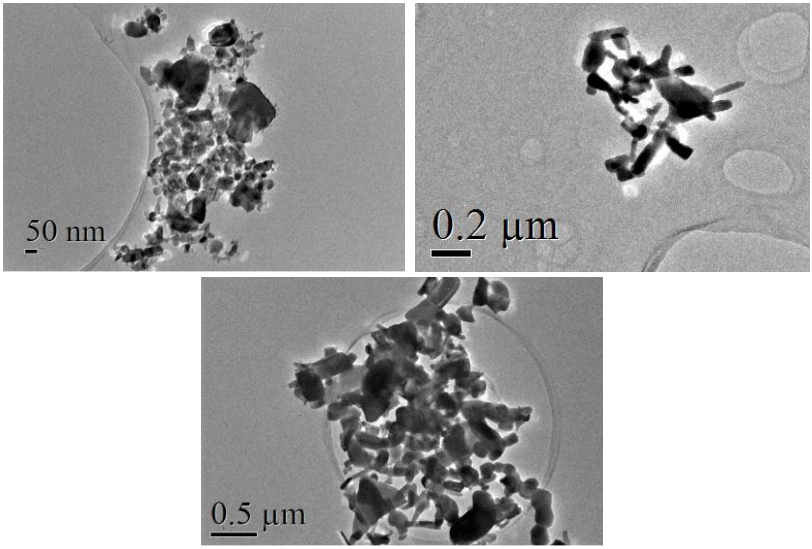

Figure 6.2. *TEM images from our particles <50nm NPs, <100nm NPs and Micro P immersed in MiliQ water.*

Figure 6.2 shows significant size dispersion among each kind of NPs, as well as completely amorphous shaping. Approximately, most of the <50nm NPs sized between 20 and 40nm (particle measures were made *in situ* through TEM), bigger particles seem to be particle clusters; <100nm NPs sized between 50-90nm, even though there can be clearly seen some particles bigger than 100nm; and Micro P mostly sized between 100 and 400nm, even though there could be found particles sizing less than 50nm.

6.4 ANTICOAGULANT

When stability studies were performed, the addition of EDTA to nanoparticle blank solutions (see Section 5.3.3, Table 5.2, Entries 1, 2 and 3) rapidly caused particle dissolution as the suspension lost its white color to the point of transparency; EDTA could not maintain our particles stable.

EDTA has much higher affinity to Zn^{2+} than to Ca^{2+} [29], thus meaning that if EDTA is able to chelate our ZnO nanoparticles. As it was observed, chelated Ca^{2+} ions would be substituted by Zn^{2+}, thus meaning that Ca^{2+} would be freed to the Plasma sample. The increase of Ca^{2+} ions in the media causes uncontrolled Plasma coagulation (Section 7.1.1.1, Table 7.1, Figure 7.1)

In contrast, when sodium citrate was added to our nanoparticle blank solutions (see Section 5.3.3, Table 5.2, Entries 4, 5 and 6) no observable change was observed.

It is known that citrate shares approximately the same affinity to Zn^{2+} than to Ca^{2+} [29] so it is expected that the chelated Ca^{2+} is not substituted for Zn^{2+} when using citrate as easily as when using EDTA, thus meaning that our ZnO particles would stay more stable when using citrate than when using EDTA.

For that reason, even though there could be potential Zn-Citrate complex formation - which due to problems with the methods of analysis (a nanometric filter was required), could not be quantified -, further studies were performed with sodium citrate as anticoagulant, instead of using EDTA.

7. PLASMA PROTEIN – ZnO INTERACTION: DISCUSSION

7.1 PLASMA COAGULATION ASSAYS

Nanoparticles are expected to interact with plasma proteins and consequently form the protein corona (see section 3.2). When bound to nanoparticles, proteins are known to lose their conformation and denaturalize (see section 3.4), thus altering metabolic processes. According to previous work [30], plasma coagulation is expected to be delayed,.

As mentioned in Section 5.4, Plasma-protein assays were performed in rat and human plasma when incubated (37ºC for 30 minutes) with ZnO nanoparticles, firstly using EDTA and eventually using sodium citrate (see section 6.4). Extrinsic pathway was studied through PT assays and Intrinsic pathway was studied through APTT assays.

7.1.1 Results from Rat Plasma Assays

7.1.1.1 EDTA as Anticoagulant

When using EDTA, the tests reported unexpected results described in Table 7.1 and represented on Figure 7.1.

As can be seen in the Extrinsic coagulation graph, the smaller the particle, the shorter is the coagulation time. This is probably caused by differences of reactivity between the particles; the smaller the particle, the higher its surface area and greater its reactivity. EDTA could be interacting more intensively with <50nm NP than with Micro P. Therefore, more chelated Ca^{2+} ions could be replaced for Zn and freed to the media to trigger plasma coagulation.

Intrinsic coagulation involves a much more complicated chain reaction. It is remarkable how <100nm NPs induced rapid coagulation while <50nm NPs never coagulated while incubating. Reasons that could cause these phenomena remain unknown.

		PT		APTT	
Entry	**Sample**	**Time (s)**	**Est. Desv. (s)**	**Time (s)**	**Est. Desv. (s)**
1	**Plasma Control**	10.0	0.93	48.5	4.9
2	**PBS Control**	10.1	1.40	56.5	5.07
3	**<50nm NP**	7.1	2.04	54.9	5.08
4	**<100nm NP**	9.2*	0.21*	0*	0*
5	**Micro P**	10.7*	0.67*	45.6*	1.05*

Table 7.1. *Coagulation time measured by prothrombin and activated partial thromboplastin time on rat plasma incubated with different sized NP's. EDTA was used as anticoagulant. Results based on 2 independent experiments of 3 replicates each. (*) Some of the replicates could not be properly studied as plasma coagulated while incubating.*

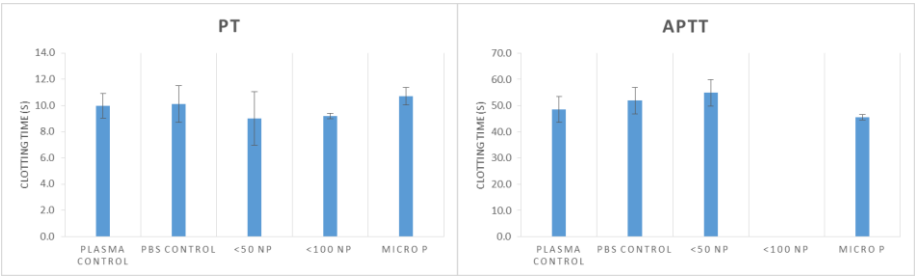

Figure 7.1. *Extrinsic and Intrinsic coagulation results from Table 7.1.*

Independent nanoparticle stability tests (see Section 6.4) stated that EDTA chelated Zn^{2+} from our nanoparticles thus freeing previously chelated Ca^{2+} ions. The freeing of Ca^{2+} ions to the media explained the uncontrolled plasma coagulation reported, as Ca^{2+} ions are essential to blood coagulation (see Section 3.3.2).

7.1.1.2 Sodium Citrate as Anticoagulant

After independent tests of particle stability when using different anticoagulants (see section 6.4), EDTA was changed into sodium citrate as anticoagulant. Results are described on Table 7.2 and represented on Figure 7.2.

		PT		APTT	
Entry	**Sample**	**Time (s)**	**Est. Desv. (s)**	**Time (s)**	**Est. Desv. (s)**
1	**Plasma Control**	8.2	0.6	21.9	1.8
2	**PBS Control**	8.2	0.8	21.3	1.7
3	**<50nm NP**	14.9	2.8	-*	-*
4	**<100nm NP**	18.8	2.4	-*	-*
5	**Micro P**	17.6	2.4	221.6 (*)	72.3 (*)

Table 7.2. *Coagulation time measured by PT and APTT on rat plasma incubated with different sized NP's. Results based on 3 independent experiments of 3 replicates each. Citrate was used as anticoagulant. (*) Not properly studied due to dispersion or absence of coagulation.*

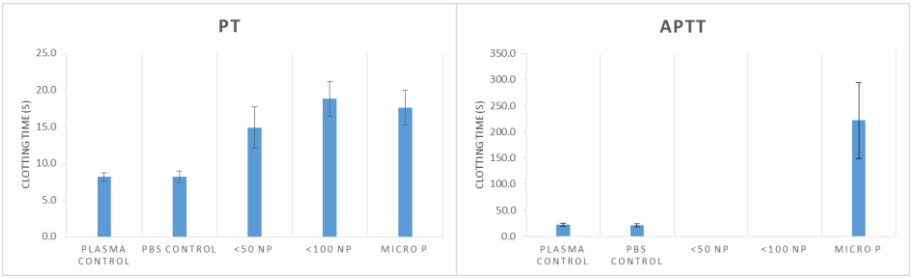

Figure 7.2. *Extrinsic and Intrinsic coagulation results from Table 7.2.*

Our findings reflect a clear effect derived from ZnO particle incubation, plasma coagulation is significantly delayed in both pathways, especially on intrinsic coagulation.

Intrinsic coagulation could not be properly studied as plasma, on most of the replicates, did not coagulate at all. The steel ball in the cuvette could freely move through the sample, thus meaning that there was no coagulation (see Section 5.4).

However, the coagulometer did stop the chronometer, with unexplainable dispersion of clotting time measurements, on some the sample replicates that apparently were not coagulated. Closer inspection of the cuvettes, once the coagulometer stopped the chronometer, revealed that little weak clots were actually formed, although they were neither big nor strong enough to trap the steel ball. Occasionally, by chance, these clots could have slightly disturbed the movement of the steel ball. When this happened, the electromagnetic sensor of the

coagulometer momentarily lost the signal of the steel ball and stopped the chronometer with great dispersion of results.

Chronometer was only stopped 3/9 times when measuring clotting time with <50nm NP samples while <100 nm NP samples did stop it in 5 of the 9 different replicates. Micro P was able to stop the chronometer 7/9 times, and even coagulated the plasma and blocked the ball's movement in 4/9 times - These last few cases are reflected in Table 5, Entry 5, as information of no statistical relevance.

The reported dispersion of results, and the impossibility to know whether some of the replicates did or did not coagulate - as the chronometer stopped although the steel ball could still move -, suggest that another methodology or instruments should be used in order, not only to quantify clotting time more precisely, but to measure clot strength as well.

7.1.2 Results from Human Plasma Assays

When using EDTA, human plasma coagulation reported similar anomalies to rat plasma; most of the samples coagulated before performing any assay, thus no significant results could be obtained.

When using sodium citrate, human plasma behaved as expected from previous studies [21], thus meaning that, once the anticoagulant was changed, the conditions of our experiments equalled those of previous studies; it is assumed that our studies are a valid continuation of this previous work.

Results obtained when using sodium citrate as anticoagulant are described in Table 7.3 and represented on Figure 7.3.

As in rat plasma coagulation assays, plasma coagulation is significantly delayed. Results obtained agree with previous work [30]; the intrinsic coagulation is the most affected pathway and, in both pathways, 50<nm NPs cause the softest effect while 100<nm NPs and micro P cause higher, similar delays on clotting time.

		PT		APTT	
Entry	**Sample**	**Time (s)**	**Est. Desv. (s)**	**Time (s)**	**Est. Desv. (s)**
1	**Plasma Control**	9.4	0.8	34.8	1.7
2	**PBS Control**	9.6	0.8	35.2	1.6
3	**<50nm NP**	18.9	0.3	373.1	44.1
4	**<100nm NP**	23.6	0.8	521.0	53.8
5	**Micro P**	21.9	0.9	522.3	57.3

Table 7.3. *Coagulation time measured by PT and APTT on human plasma incubated with different sized NP's. Results based on 2 independent experiments of 3 replicates each. Citrate was used as anticoagulant.*

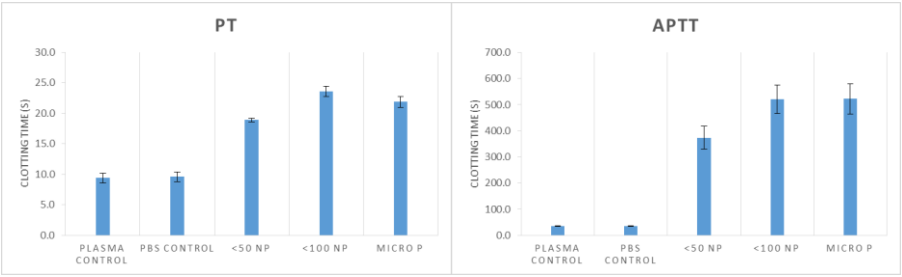

Figure 7.3. *Extrinsic and Intrinsic coagulation results from Table 7.3.*

It is stated that the stimulation of the intrinsic coagulation pathway and nanoparticle size could be proportionally correlated [31] - meaning that the bigger the particle, the earlier plasma should coagulate – although this has only been found to apply in SiO_2 particles. Our findings did not agree with this statement as they displayed reverse relation.

Similar to rat plasma assays, clots formed when measuring APTT on some replicates was only enough to stop the chronometer from our coagulometer, but not to completely block the movement of the steel ball. This was reported to happen a couple of times when using <50nm NPs. As stated when discussing rat plasma results, these anomalies suggest the use of other methodologies or instruments in order to improve the reliability of our results from these assays.

7.1.3 Comparison between Rat and Human Coagulation

Results for extrinsic coagulation reported similar results for both rat and human studies. In contrast, there could be observed great differences when measuring clotting time on the intrinsic coagulation cascade; rat's intrinsic pathway was not just slowed as human's, but completely obstructed. Moreover, their behaviour seems inversed. In human plasma, coagulation time increases in parallel with particle size whereas in the case of rat plasma coagulation is observed only when incubated with Micro P, but not in the presence of smaller sized nanoparticles that apparently impeded the coagulation.

It should be noted that different behaviour between rat and human plasma is to be expected even in regular conditions [32]. One of the possible reasons for these changes is that rat plasma contains slightly lower concentration of fibrinogen and other important coagulating factors [33], thus meaning that higher relative quantity of coagulation proteins could be trapped, and deactivated, by the NP.

Another reason that could explain these results is that rat and human plasma proteins, like fibrinogen, are not identical [34][35], thus potentially contributing to behavioural differences in front of ZnO NPs.

In conclusion, equivalence between rat and human studies on ZnO nanotoxicity studies remains uncertain. Further studies should be adapted depending on the organism on which the study is performed. Anyway, differential behaviour between organisms could provide different perspectives to study the effects of ZnO nanoparticle absorption.

7.2 Protein Quantification Assays

Although protein quantification assays were only meant to be orientative tests to optimize SDS-PAGE, results obtained from NP's pellets were of significant value, as described in Table 7.4.

Entry	Solution	[Total protein] Human plasma (mg/ml)	[Total protein] Rat plasma (mg/ml)
1	PBS Control	52777.6	44099.5
2	<50nm NP – Pel*	681.5	670.0
3	<100nm NP – Pel*	364.3	435.0
4	Micro P – Pel*	177.9	205.8

Table 7.4. *Total protein concentration measured in pellets from different sized NPs incubated in human or rat plasma. Sodium citrate was used as anticoagulant. *Pel: particles' pellet.*

It is stated that differential behaviour among NPs could be attributed on their size -and so of particle curvature and surface area [19]. This statement agrees with our data, as a clear correlation between total protein adsorbed by the NP's and their size is observed; as the particle size diminishes, surface area and particle curvature increase and so does the total amount of protein adsorbed. This data will help to understand the results from the following SDS-PAGE and TEM assays.

7.3 SDS-PAGE ASSAYS

7.3.1 Human Gels Discussion

Herein, only the most abundant proteins with characteristic and easy recognized stained bands, such as albumin and fibrinogen, could be reliably identified. For deeper understanding of the proteins adsorbed in the particles, gel digestion and further analytical assays should be performed. Moreover, these analyses could provide crucial information in order to understand the Protein-Particle interaction and predict potential physiological alterations.

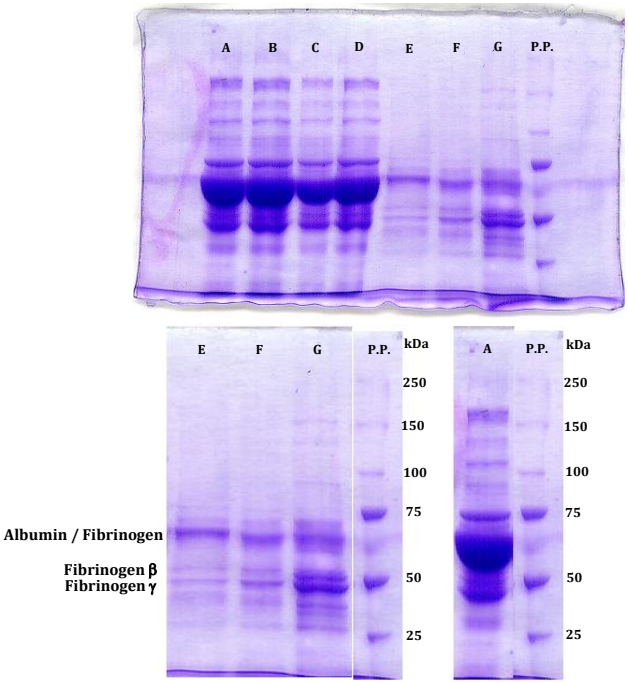

Figure 7.4. *SDS-PAGE Human plasma. (A) Plasma Control; (B) Micro P, SN; (C) <100nm NP, SN; (D) <50nm NP, SN; (E) Micro P, Pellet; (F) <100nm NP, Pellet; (G) <50nm NP, Pellet; (P.P.) Protein pattern. Approximated protein amount injected from pellets was 4μg for A, B and C.*

Our findings show how certain proteins were adsorbed on the NPs with greater affinity than others. For instance, in Figure 7.4 (G, <50nm NPs pellet), the stained protein bands corresponding to fibrinogen β and γ (due to reduction, fibrinogen breaks into 3 different subunits: α, β, γ; see Section 5.5.2) are greater than the one of albumin, thus meaning that fibrinogen is present in greater concentration in the protein corona. Note that, in normal conditions, human plasma albumin is found in concentrations 20 times higher than fibrinogen (see section 3.3.1) as it can be observed in the control track (Figure 7.4, track A) which reveals a great stain band mainly constituted by albumin while the ones from fibrinogen β and γ remain regular sized. In conclusion, it can be assumed that fibrinogen has more affinity to ZnO NPs than albumin, especially to <50nm NPs. It should be noted that the albumin-fibrinogen relation varies with particle size, Track E (Micro Ps pellet) shows more albumin than fibrinogen.

Fibrinogen presence on the protein corona could explain the delays on plasma coagulation reported on Section 7.1; if fibrinogen is trapped in the protein corona, it cannot perform its coagulation role as ZnO particles could be deactivating or denaturalizing it, as reported in previous studies to happen to numerous proteins (see Section 3.4). Even though, this would imply that the particles that adsorbed the most fibrinogen caused the greatest delays of plasma coagulation, which contradicts our findings on Section 7.1. Micro Ps seem to adsorb less fibrinogen, although their effects on plasma coagulation were more significant than <50nm NPs, that seemed to adsorb more fibrinogen. This suggests, as previously stated, the importance of further analysis and gel digestion, in order to accurately know each protein that was adsorbed on the particles that could alter physiological processes like plasma coagulation.

Even though other proteins could not be identified, some band stains could be qualitatively compared as represented in Table 7.5.

Approx. MW stain (kDa)	**<50 nm NP**	**<100 nm NP**	**Micro P**	**control**
46 (Fibrinogen γ)	++	++	+	+++
52 (Fibrinogen β)	++	++	+	+++
66 (Fibrinogen α / Albumin)	++	++	++	+++
≈70	++	+	+	++
≈75	-	+	+	++
≈90	+	-	-	+
≈110	-	-	-	+
≈135	+	+	-	+
≈150	+	-	-	+
≈160	-	-	-	++

Table 7.5. *Qualitative comparison of present protein stained bands in each particle track and plasma control from Figure 7.4 using human plasma. (+++) Great presence; (++) Significant presence; (+) Slightly present; (-) Apparently absent.*

Differences among NPs sizing are well observed. For instance, Track G from Figure 7.4 reveals much greater fibrinogen γ and β stains than Track F and E, thus meaning that fibrinogen has much more affinity to <50nm NPs than it does to the other particles. Moreover, most stains seem to pale as particle size grows, as global protein-particle affinity lowers with

bigger particles (see Section 7.2), although it is not the case for albumin/fibrinogen α stain that seems to gain significance.

7.3.2 Rat Gels Discussion

In parallel with human gels, only the most characteristic protein stain bands could be recognized without gel digestion and further analytical assays. This time, only albumin could be reliably identified within the pellet tracks whereas fibrinogen seemed to remain absent, thus meaning that possible differences in protein conformation (see Section 7.1.3) could provoke crucial adsorption differences. SDS- PAGE gels of rat plasma can be observed in Figure 7.5.

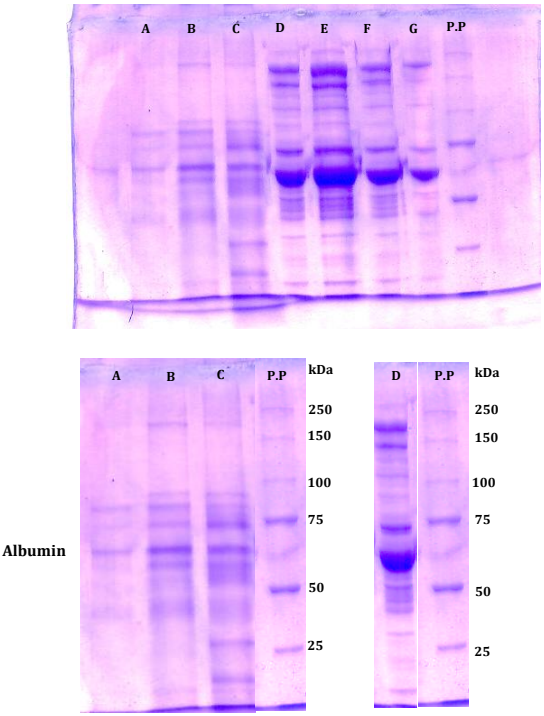

Figure 7.5. *SDS-PAGE Rat plasma. (A) Micro P, Pellet; (B) <100nm NP, Pellet; (C) <50nm NP, Pellet; (D) Plasma Control; (E) Micro P, SN; (F) <100nm NP, SN; (G) <50nm NP, SN; (P.P.) Protein pattern. Approximated protein amount injected from pellets was 8μg for C and B and 4μg for A.*

It should be noted that while in human gels it was mostly seen disappearance of stained bands, rat gels show the appearance of certain bands. <50nm NPs show a couple of significant stained bands of approximately ≈27 and ≈15 kDa that did only slightly appear in the control track, and all three particle tracks show the appearance of one band at approximately ≈85kDa that neither did appear in the control track. It is concluded that this bands are composed by proteins that are greatly adsorbed in our particles, thus significantly concentrating them in the pellet tracks while in regular rat plasma are found in diminutive amounts.

Herein, Micro P's track cannot be adequately compared to NPs' tracks as it was not possible to concentrate them enough to inject the same amount of protein. However, there were found some differences between <50 and <100nm NPs. ≈15 and ≈27 kDa protein stained bands were only found in <50nm NPs and while the ≈72 kDa stain band is greater in <50nm NPs, ≈200kDa stain band is greater in <100nm NPs.

As can be observed in rat plasma gels, in contrast with human plasma gels, albumin could be identified but fibrinogen was not. Rat fibrinogen breaks into different pieces compared to human fibrinogen; band stains from rat fibrinogen β and α weight the same (approximately 47 kDa), and fibrinogen δ weights around 52 kDa [35]. Neither of these protein stain bands could be observed in our gels.

The absence of fibrinogen trapped in the protein corona leaves us to suppose that delays on rat plasma coagulation could be rather caused by adsorption of other relevant coagulation factors instead of fibrinogen – in contrast with human plasma. Therefore, further analytical assays are essential to fully understand and discuss our findings, as previously stated.

Once again, even though most proteins could not be identified, some band stains could be qualitatively compared as represented in Table 7.6.

Approx. MW stain (kDa)	<50 nm NP	<100 nm NP	Micro P	control
≈12	+	+	+	++
≈15	++	-	-	+
≈27	++	-	-	+
47 (Fibrinogen γ)	NC	NC	-	+
52 (Fibrinogen α/β)	NC	NC	-	+
66 (Albumin)	++	+	+	+++
≈72	++	+	+	++
≈85	+	+	+	-
≈90	+	+	+	+
≈110	-	-	-	+
≈145	-	-	-	++
≈200	+	+	+	++

Table 7.6. *Qualitative comparison of present protein stained bands in each particle track and plasma control from Figure 7.5 using rat plasma. (+++) Great presence; (++) Significant presence; (+) Slightly present; (-) Apparently absent; (NC) Not Clear enough.*

7.3.3 General Comparison

SDS-PAGE gels revealed different protein-NPs affinity profiles depending on the source of plasma or particle size, as can be observed in Figures 7.4 and 7.5.

Differences among supernatants (Figure 7.4, tracks B, C, D; Figure 7.5, tracks D, F, G) can't be identified as they lie upon the amount of proteins removed by the NPs from the original media, which is diminutive in comparison with the total amount of proteins that remain present in the sample. Possible experimental errors could suppose greater difference.

Moreover, differences depending on the organism studied are well observed. As previously stated (see Section 7.1.3), plasma proteins from humans and rats are not identical, the conformations can differ thus provoking changes in their affinity to these NPs. For instance, most of human gel's stained bands were found between 25 and 75kDa, while in rat gels stained bands were found all along the tracks.

7.4 TEM STUDIES: PROTEIN CORONA

When immersed in plasma, TEM observations revealed protein accumulations around our particles, as can be seen in Figures 7.6, 7.7 and 7.8. Black spots correspond to particles and shadowy staining corresponds to plasma proteins. These findings should be compared to those on Section 6.3.

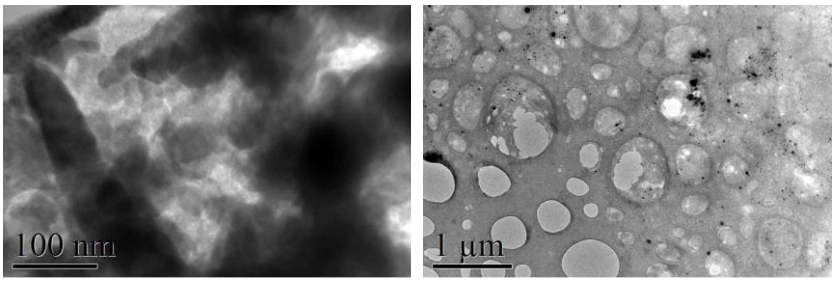

Figure 7.6 *Images taken from plasma incubated <50nm NPs.*

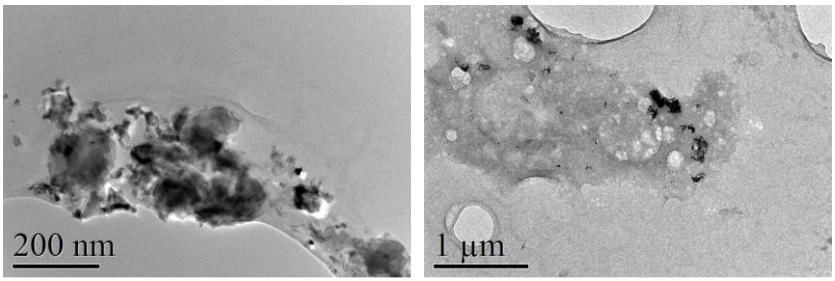

Figure 7.7 *Images taken from plasma incubated <100nm NPs.*

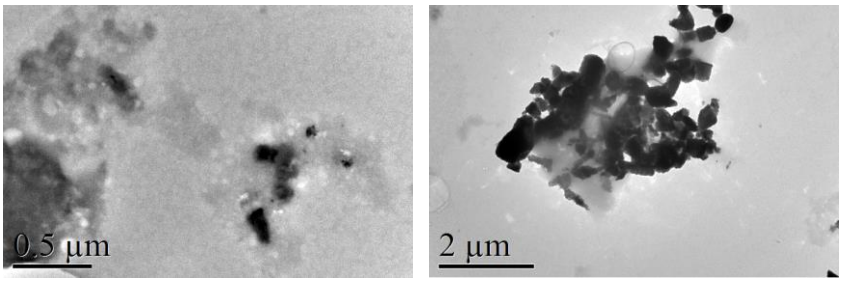

Figure 7.8 *Images taken from plasma incubated Micro Ps.*

Organic substances are degraded by the electron beam while the observation takes place; as time went by, nanoparticles seemed to move as the surrounding proteic media that coated them was altered. Altogether, this degradation process proved protein presence.

Protein presence was corroborated by elemental analysis (EDX) from the same TEM instrument. As can be seen in figure 7.9 as an example, shadowy staining around the particles from figures 7.6 to 7.8 reported presence of tungsten (see Section 5.6).

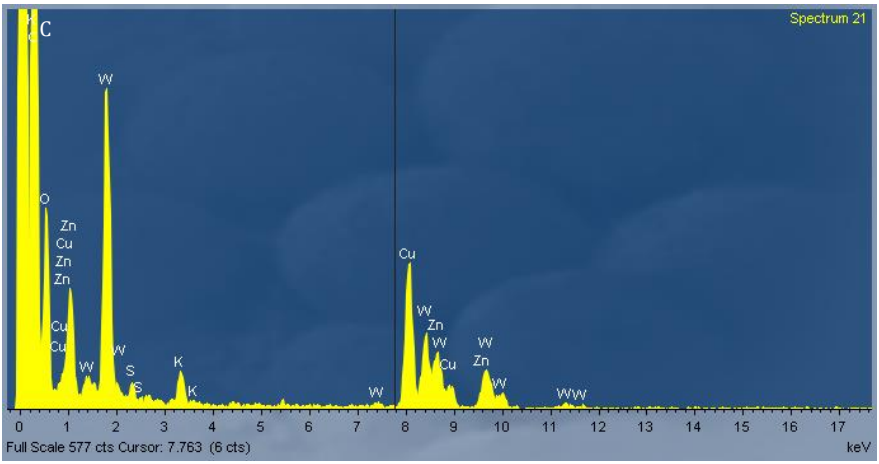

Figure 7.9 *Elemental analyses from particles on the right picture from Figure 7.6. Presence of tungsten (W peaks) reveals protein presence that is corroborated, by C and S peaks. Zn peaks confirm the presence of our particles. Cu peaks correspond to the sample grid K peaks come from staining.*

Differences among particles were significant. <50nm NPs revealed large and dense stains of protein where our particles where immersed. Sometimes our particles could not be found within the stains. <100nm NPs displayed similar behaviour, although protein stains were lighter and clearer coating around the particles could be observed. On the other hand, Micro P revealed clear protein coating. No individual protein stains were found on Micro P samples. These phenomena agree with our findings and conclusions from Section 7.2.

8. CONCLUSIONS

Following the objectives set on the beginning of our studies it can be concluded that:

1. ZnO particles could be characterized. Our particles displayed total amorphous shaping and significant dispersion of particle size. When immersed in aqueous media, ZnO particles agglomerated rapidly, although that agglomeration was palliated when immersed in plasma.

2. Blood coagulation profiles between rat and human plasma when incubated with ZnO particles proved to be significantly different when measuring the Intrinsic coagulation pathway. Rat's blood intrinsic pathway was completely obstructed, in contrast with human's intrinsic pathway – only delayed. Extrinsic pathway was found to be similarly affected. Nevertheless, another methodology should be used in order to perform more adequate studies.

3. SDS-PAGE gels displayed clear differences in plasma protein-particle affinities depending upon species studied and particle size. Further deeper analytical assays should be performed in order to determine which proteins were adsorbed in each particle - and which ones did not -, therefore revealing common characteristics among the adsorbed proteins that could help understand and predict protein corona's formation and behavior.

4. Protein corona presence was visually confirmed on TEM observations and its quantitative presence – it was more present in <50nm NPs samples than in Micro P samples - was allied to our other findings.

9. REFERENCES AND NOTES

[1] M. A. Maurer-Jones, S. A. Love, S. Meierhofer, B. J. Marquis, Z. Liu, and C. L. Haynes, "Toxicity of nanoparticles to brine shrimp: An introduction to nanotoxicity and interdisciplinary science," *J. Chem. Educ.*, vol. 90, no. 4, pp. 475–478, 2013.

[2] J. D. Heidel and M. E. Davis, "Clinical developments in nanotechnology for cancer therapy," *Pharm. Res.*, vol. 28, no. 2, pp. 187–199, 2011.

[3] R. Pati, R. K. Mehta, S. Mohanty, A. Padhi, M. Sengupta, B. Vaseeharan, C. Goswami, and A. Sonawane, "Topical application of zinc oxide nanoparticles reduces bacterial skin infection in mice and exhibits antibacterial activity by inducing oxidative stress response and cell membrane disintegration in macrophages.," *Nanomedicine*, vol. 10, no. 6, pp. 1195–208, 2014.

[4] M. Premanathan, K. Karthikeyan, K. Jeyasubramanian, and G. Manivannan, "Selective toxicity of ZnO nanoparticles toward Gram-positive bacteria and cancer cells by apoptosis through lipid peroxidation.," *Nanomedicine*, vol. 7, no. 2, pp. 184–92, 2011.

[5] M. Vaseem, A. Umar, and Y. Hahn, *ZnO Nanoparticles : Growth , Properties , and Applications*, vol. 5, no. January. 1988.

[6] Y. Li, Y. Zhang, and B. Yan, "Nanotoxicity overview: Nano-threat to susceptible populations," *Int. J. Mol. Sci.*, vol. 15, no. 3, pp. 3671–3697, 2014.

[7] Z. J. Deng, G. Mortimer, T. Schiller, A. Musumeci, D. Martin, and R. F. Minchin, "Differential plasma protein binding to metal oxide nanoparticles.," *Nanotechnology*, vol. 20, no. 45, p. 455101, 2009.

[8] S. Tenzer, D. Docter, J. Kuharev, A. Musyanovych, V. Fetz, R. Hecht, F. Schlenk, D. Fischer, K. Kiouptsi, C. Reinhardt, K. Landfester, H. Schild, M. Maskos, S. K. Knauer, and R. H. Stauber, "Rapid formation of plasma protein corona critically affects nanoparticle pathophysiology.," *Nat. Nanotechnol.*, vol. 8, no. 10, pp. 772–81, 2013.

[9] K.-M. Kim, M.-H. Choi, J.-K. Lee, J. Jeong, Y.-R. Kim, M.-K. Kim, S.-M. Paek, and J.-M. Oh, "Physicochemical properties of surface charge-modified ZnO nanoparticles with different particle sizes.," *Int. J. Nanomedicine*, vol. 9 Suppl 2, pp. 41–56, 2014.

[10] S. L. Hirsh, D. R. McKenzie, N. J. Nosworthy, J. A. Denman, O. U. Sezerman, and M. M. M. Bilek, “The Vroman effect: competitive protein exchange with dynamic multilayer protein aggregates.,” *Colloids Surf. B. Biointerfaces*, vol. 103, pp. 395–404, 2013.

[11] G. J. Tortora and B. Derrickson, *Principios de Anatomía y Fisiología*, 11th ed. Buenos Aires: Editorial Médica Panamericana, 2006.

[12] T. Farrah, E. W. Deutsch, G. S. Omenn, D. S. Campbell, Z. Sun, J. A. Bletz, P. Mallick, J. E. Katz, J. Malmström, R. Ossola, J. D. Watts, B. Lin, H. Zhang, R. L. Moritz, and R. Aebersold, “A high-confidence human plasma proteome reference set with estimated concentrations in PeptideAtlas.,” *Mol. Cell. Proteomics*, vol. 10, no. 9, p. M110.006353, 2011.

[13] N. W. Tietz, *Fundamentals of Clinical Chemistry*, 2nd ed. Philadelphia, PA: W. B. Saunders Company, 1976.

[14] K. T. Preissner, “Biological relevance of the protein C system and laboratory diagnosis of protein C and protein S deficiencies,” *Clin. Sci.*, no. 78, pp. 351–364, 1990.

[15] P. C. Harpel, “Studies on human plasma alpha 2-macroglobulin-enzyme interactions. Evidence for proteolytic modification of the subunit chain structure.,” *J. Exp. Med.*, vol. 138, no. 3, pp. 508–21, 1973.

[16] M. H. Coan and R. C. Roberts, “A redetermination of the concentration of alpha 2-macroglobulin in human plasma.,” *Biol. Chem. Hoppe. Seyler.*, vol. 370, no. 7, pp. 673–6, 1989.

[17] S. Palta, R. Saroa, and A. Palta, “Overview of the coagulation system,” *Indian J. Anaesth.*, vol. 58, no. 5, p. 515, 2014.

[18] G. J. Pillai, M. M. Greeshma, and D. Menon, “Impact of poly(lactic-co-glycolic acid) nanoparticle surface charge on protein, cellular and haematological interactions.,” *Colloids Surf. B. Biointerfaces*, vol. 136, pp. 1058–66, 2015.

[19] N. Durán, C. P. Silveira, M. Durán, and D. S. T. Martinez, “Silver nanoparticle protein corona and toxicity: a mini-review.,” *J. Nanobiotechnology*, vol. 13, no. 1, p. 55, 2015.

[20] A. K. Bhunia, P. K. Samanta, S. Saha, and T. Kamilya, “ZnO nanoparticle-protein interaction: Corona formation with associated unfolding,” *Appl. Phys. Lett.*, vol. 103, no. 14, 2013.

[21] L. Marics, “Comparative study of zinc oxide hemocompatibility at nano- and micrometric scale. (TFG),” Universitat de Barcelona, 2015.

[22] “Zinc oxide | 1314-13-2.” [Online]. Available: http://www.chemicalbook.com/ChemicalProductProperty_EN_CB3853034.htm. [Accessed: 06-May-2016].

[23] T. Meißner, K. Oelschlägel, and A. Potthoff, “Implications of the stability behavior of zinc oxide nanoparticles for toxicological studies,” *Int. Nano Lett.*, vol. 4, no. 3, p. 116, 2014.

[24] A. Dhawan and V. Sharma, “Toxicity assessment of nanomaterials: methods and challenges.,” *Anal. Bioanal. Chem.*, vol. 398, no. 2, pp. 589–605, 2010.

[25] M. A. Dobrovolskaia and B. W. Neun, *NCL Method ITA-12. Coagulation Assays.* Nanotechnology Characterization Laboratory, 2006.

[26] G. A. Tennent, S. O. Brennan, A. J. Stangou, J. O’Grady, P. N. Hawkins, and M. B. Pepys, “Human plasma fibrinogen is synthesized in the liver.,” *Blood*, vol. 109, no. 5, pp. 1971–4, 2007.

[27] “Introduction to PAGE | Sigma-Aldrich.” [Online]. Available: http://www.sigmaaldrich.com/technical-documents/articles/biology/sds-page.html. [Accessed: 15-Apr-2016].

[28] W. M. Ibrahim, A. H. AlOmrani, and A. E. B. Yassin, “Novel sulpiride-loaded solid lipid nanoparticles with enhanced intestinal permeability.,” *Int. J. Nanomedicine*, vol. 9, pp. 129–44, 2014.

[29] R. M. Smith and A. E. Martell, “Critical stability constants, enthalpies and entropies for the formation of metal complexes of aminopolycarboxylic acids and carboxylic acids,” *Sci. Total Environ.*, vol. 64, no. 1–2, pp. 125–147, 1987.

[30] P. Vilardell, L. Marics, and M. Mitjans, “Comparative study of zinc oxide hemocompatibility at nano- and micrometric scale.,” Universitat de Barcelona, 2015.

[31] T. Kushida, K. Saha, C. Subramani, V. Nandwana, and V. M. Rotello, “Effect of nano-scale curvature on the intrinsic blood coagulation system,” *R. Soc. Chem.*, no. 6, pp. 14484–14487, 2014.

[32] J. M. Siller-Matula, R. Plasenzotti, A. Spiel, P. Quehenberger, and B. Jilma, “Interspecies differences in coagulation profile,” *Thromb. Haemost.*, vol. 100, no. 3, pp. 397–404, 2008.

[33] A. García-Manzano, J. González-Llaven, C. Lemini, and C. Rubio-Póo, “Standardization of rat blood clotting tests with reagents used for humans.,” *Proc. West. Pharmacol. Soc.*, vol. 44, pp. 153–5, 2001.

[34] R. F. Doolittle and J. M. Kollman, “Natively unfolded regions of the vertebrate fibrinogen molecule,” *PROTEINS Struct. Funct. Bioinforma.*, vol. 63, pp. 391–397, 2006.

[35] H. Bouma III and G. M. Fuller, “Partial Chemical Characterization of Rat Fibrinogen,” *Biol. Chem.*, vol. 250, no. 12, pp. 4678–4683, 1975.

10. ACRONYMS

SDS Sodium Dodecyl Sulphate

PAGE Polyacrylamide Gel Electrophoresis

NP Nanoparticle

SN Supernatant

ATPP Activated Partial Thromboplastin time

PT Prothrombin Time

EDTA Ethylenediaminetetraacetic acid

TEM Transmission electron microscopy

PBS Phosphate-buffered saline

MW Mass Weight

EDX Energy-dispersive X-ray spectroscopy